International Journal of Advanced Technology and Engineering Exploration, Vol 12(122)
ISSN (Print): 2394-5443 ISSN (Online): 2394-7454
http://dx.doi.org/10.19101/IJATEE.2024.111100212

Research Article

Durability and microstructural analysis of self-compacting concrete with ternary blends exposed to sulphate environment

Amrendra Singh*, Rakesh Kumar, P. K. Mehta and Pawan Kumar
Department of Civil Engineering, Motilal Nehru National Institute of Technology Allahabad, Prayagraj-211004, Uttar Pradesh, India

Received: 26-February-2024; Revised: 22-January-2025; Accepted: 25-January-2025

Abstract
For sustainable infrastructural development, the massive generation of waste materials such as fly ash (FA), rice husk ash (RHA), and stone dust (SD) has made their utilization in the production of self-compacting concrete (SCC) a matter of prime research importance. Due to their pozzolanic qualities, FA and RHA may be utilized as partial replacements for cement in several construction activities. On the other hand, SD a waste product from a stone crusher plant, increases density and possesses strong compressive strength when used in concrete production due to its properties. Replacing natural sand (N-sand) with SD may help achieve sustainability objectives. This study examined the durability characteristics of SCC, which are made by optimizing SD for N-sand and (FA+RHA) for ordinary Portland cement (OPC). Several tests were carried out to evaluate the fresh and hardened properties of the specimen prepared. After optimizing the proportions of FA, FA+RHA, and FA+RHA+SD, three types of SCC mixes were prepared: SCC-I (80% OPC + 20% FA + 100% N-sand), SCC-II (75% OPC + 20% FA + 5% RHA + 100% N-sand), and SCC-III (75% OPC + 20% FA + 5% RHA + 65% N-sand + 35% SD). These mixes were exposed to an ammonium sulphate [$(NH_4)_2SO_4$] solution with a concentration of 4.0 grams/liter for up to 360 days for durability analysis. All specimens were subsequently subjected to microstructural analysis. The obtained results were compared and analyzed. It was observed that after 56 days of exposure, the sorptivity of SCC-III decreased by 7.43% and 34.50% compared to SCC-II and SCC-I, respectively. After 360 days, the reduction in sorptivity was 9.25% and 40.24%, respectively, when compared to SCC-II and SCC-I. The results of this study pave the way for using SCC in construction activities to achieve society's sustainability goals.

Keywords
Self-compacting concrete, Fly ash, Rice husk ash, Stone dust, Sustainability, Durability analysis.

1.Introduction
One of the world's most extensively utilized building materials is concrete, which leads to cement production due to an increase in infrastructural development [1]. The production of ordinary Portland cement (OPC) causes a significant release of carbon dioxide (CO_2) which is harmful to the environment due to its greenhouse effects [2] Severe air pollution has been observed due to an increase in CO_2 emissions due to increment through production [3]. Studies have shown that one tonne of OPC clinker produces about one tonne of CO_2 [4]. On the other hand, sustainable building materials should have a minimum adverse impact on the environment [5].

Bagasse ash, wood ash, natural pozzolans, silica fume (SF), rice husk ash (RHA), and other comparable pozzolanic materials can be used to make concrete more durable while using less OPC [6]. Environmental problems are taking place due to the extensive usage of natural sand (N-sand), which also depletes natural resources on a large scale [7]. Due to growing environmental concerns and agreements to prioritize environmental protections, the government has put restrictions on N-sand mining from riverbeds [8]. To solve these problems, it is necessary to use affordable alternative materials without sacrificing other quality standards for constructing heavy structures. Self-compacting concrete (SCC) is being utilized more frequently in the building sector due to its higher strength, even in sophisticated places [9]. The SCC has more fine particles, a higher dosage of admixtures, and a more optimal packing density than

*Author for correspondence

ordinary concrete, which results in the necessary fluidity and viscosity [10]. It has been demonstrated that adding very fine particles to concrete improves both its mechanical and physical qualities [11]. The SCC demonstrates excellent passage, filling, and segregation resistance. Various pozzolanic materials, including fly ash (FA), ground granulated blast-furnace slag (GGBS), Metakaolin (MK), RHA, and others, are used to create SCC in general [12, 13]. This approach addresses the challenge of safely disposing of these waste materials, making construction more sustainable and resulting in environmentally friendly concrete mixtures. FA constitutes 20% to 40% (by weight) of the raw coal used in thermal power plants. Globally, approximately 25% of FA production is utilized, with 38% in India and 47% in the European Union [14, 15]. The worldwide production of FA and RHA is illustrated in *Figure 1* [16, 17].

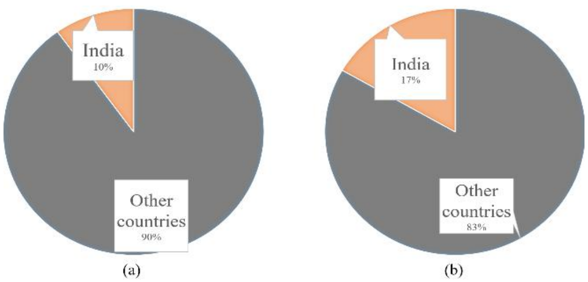

Figure 1 Production of (a) FA and (b) RHA worldwide and in India

This study significantly contributes to advancing sustainable construction practices by demonstrating the effective utilization of industrial waste materials such as FA, RHA, and SD in SCC production. The research provides a comprehensive evaluation of the workability, durability, and microstructural properties of SCC mixes, emphasizing their performance under aggressive sulphate exposure. By optimizing the proportions of FA, RHA, and SD, the study showcases their potential to enhance SCC's fresh and hardened properties while reducing environmental impact. The microstructural analysis offers critical insights into the role of CSH gel formation and pore structure refinement, which improve sulphate resistance and long-term performance. These findings pave the way for adopting sustainable materials in high-performance concrete, addressing waste disposal challenges, and contributing to global sustainability goals in construction.

This paper is organized as follows: Related work is discussed in Section 2, followed by Materials and Methods in Section 3. The Results are presented in Section 4, while the Discussion of the results and their implications is covered in Section 5. Finally, the paper is concluded in Section 6.

2.Literature reviews

Several studies have demonstrated the potential of utilizing FA and RHA in concrete production. FA, in particular, has shown an additional beneficial impact on the compressive and flexural strength of concrete due to its pozzolanic behavior [18]. Substituting 15% of OPC with FA has been found to enhance the strength parameters of SCC. Moreover, cost-effective SCC can be produced using significant amounts of Class f-FA [15]. The flowability of SCC mixes improved significantly when ultra-pulverized FA was used as a partial replacement for OPC, with V-funnel times falling within the limits set by the European Federation of National Associations Representing Concrete (EFNARC) [19]. Replacing 30% of OPC with FA was proven to yield excellent results in terms of workability, mechanical characteristics, and durability [20]. Another study demonstrated that laterized concrete mixes containing steel fibers and FA exhibited better mechanical properties than ordinary concrete. An optimum mix ratio of 25% granite aggregates, 5% FA, 0.5% steel fibers, and 1.6% superplasticizer (SP) was identified [21]. The qualities of the cement and admixtures used significantly influence the properties of SCC, with even minor adjustments having a considerable impact. For example, the addition of FA generally increased the slump values, particularly when combined with SP [22].

The study found that the fresh density of the concrete decreased when more FA was used in place of cement. The 60% FA mixture had the lowest T50 slump flow times, while the control mixture had the greatest. FA replacement led to a continuous decrease in compressive strength over time, but it also made the SCC blends more passable than other mixes [23]. The study shows that traditional cement-based and alkali-activated slag-based mortars have comparable water capillary absorption properties. The mortar made of 50% FA and 50% slag, created with the least amount of NaOH, had the least negative effects on the environment. After 28 and 90 days of curing, the mortar comprising 75% slag and 25% FA with a slag to FA ratio of 3:1, demonstrated increased compressive strength. It also exhibited the lowest initial rate of water absorption [24]. RHA's chemical and physical characteristics make it an appropriate supplemental cementitious material for producing ultra-high-performance concrete (UHPC). Nevertheless, because it results in a higher volume paste and less available free water, increasing the RHA percentage can make the fresh UHPC combination less flowable. The compressive strength of UHPC is slightly reduced by adding mineral admixture to lower the cement content, but the concrete's carbon footprint is much reduced [25]. Water negatively affects compressive strength; however, there is a strong correlation between water content and RHA, indicating that higher water levels are required to enhance resistance when RHA is used [25]. Without causing any adverse effects, SCC's durability can be increased by substituting up to 40% of OPC with a mixture of RHA and MK. Unlike unblended SCC, blended SCC composites with 30% MK exhibit better strength and permeability. Nevertheless, MK-blended SCC performs poorly in acidic settings. RHA-blended SCC exhibits better durability and lower compressive strength, particularly against acid attack [26]. Although the workability of concrete is not significantly affected by using RHA and MK, it can be enhanced by adding more water-reducing admixture. RHA does not negatively impact compressive strength up to 15-20%. However, SCC strength can increase by up to 25% when 15% MK is applied. The optimal compressive strength was achieved with a mix containing 15% MK and 10% RHA replacements. Concrete's higher compressive strength can be explained by a more homogenous structure and greater production of a calcium silicate hydrate (CSH) gel, as revealed by x-ray diffraction (XRD) and scanning electron microscopy (SEM) examination [27].

At different doses, adding nano rice straw ash (NRSA) o concrete has been demonstrated to increase compressive strength; after seven to ninety days of curing, a notable improvement in strength has been observed. Strong CSH peaks were found by Raman spectroscopy, while weak calcium hydroxide (CH) and ettringite peaks were identified by X-ray analysis [28]. The high density and low pores prevented pitting corrosion, and the presence of nanomaterials improved charge transfer resistance and concrete bulk resistance [28]. By weight of the rice, 20–25% of rice husks are produced throughout the world [29]. Burning rice husk results in the removal of cellulose and lignin, leaving just silica ash [30]. RHA is composed chemically of 82–95% silica at controlled burning temperatures of 600–800°C [31, 17]. Several studies have found that when the water/binder (w/b) ratio is decreased, the slump flow of mortar decreases and the flow durations of SCC increase as the RHA percentage increases [32]. When RHA partially replaces OPC; as a result, the paste volume increases, the density of RHA decreases, and the slump flow increases. The V-funnel duration increases, and the slump flow reduces with the same dose of SP as the concentration of RHA increases [32].

On the other hand, most emerging nations are forced by government policies to minimize the consumption of fine aggregate in concrete with another material, either totally or partially, without compromising the quality of the concrete [33]. In the construction sector, Stone dust (SD) has been used in various application, such as aggregates, bricks, tiles, building materials, and materials for road development [34]. It has significant potential to replace fine materials, such as sand, construction industry, which will reduce the cost of construction and conserve the natural resources of construction materials in the environment [35]. Numerous findings indicate that SD-produced concrete has strength characteristics that are almost identical to those of conventional concrete. It has been found that replacing up to 40% of the fine aggregates in concrete with SD has little effect on its compressive strength, but it greatly increases its flexural strength throughout its lifetime [36]. As the percentage of SD in concrete increases, its permeability decreases [37]. The cost of concrete can be reduced by increasing the percentage of SD. Concrete's compressive and flexural strength can be increased by up to 70% using stone processing dust, a fine aggregate with better water absorption properties. It improves elasticity modulus by minimizing voids and strengthening the binding between cement paste and aggregate. Dust from stone processing has a detrimental effect on abrasion resistance but has no discernible effect on impact resistance. It also reduces the depth of water penetration in concrete. The economics of concrete can be increased by using stone processing dust as a fine aggregate [38]. Waste from stone production can compete with sand and limestone filler as an environmentally friendly substitute for cement based on civil construction materials. It can lessen the environmental effect of masonry, rendering mortars, and SCC by partially substituting sand in combinations [39].

3.Materials and Methods

3.1Materials used

To carry out this study, the OPC, RHA, FA, N-sand, SD and the coarse aggregate of size 10 to 20 mm, potable water and SP have been used. The physical and chemical characteristics of these materials have been evaluated.

3.1.1Ordinary portland cement (OPC)

It has been collected from a local distributor in Prayagraj Uttar Pradesh, India. The physical characteristics of OPC grade 43 have been presented in *Table 1*. Ensure the cement is free from lumps and stored properly to prevent moisture absorption. The compressive strength test of OPC, at three, seven, and twenty-eight days, was calculated by performing standard tests as per Indian Standards (IS-8112:2013), as shown in *Table 1*.

Table 1 Physical properties of OPC (grade 43)

Properties	Values
OPC Grade	43
Consistency	27%
Specific gravity	3.14
Fineness modulus	1.4%
Soundness	2.0 mm
Initial setting time	60 minutes
Final setting time	480 minutes
Compressive strength at 03 days	24.09 N/mm^2
Compressive strength at 07 days	34.33 N/mm^2
Compressive strength at 28 days	48.67 N/mm^2

The chemical composition of OPC (grade 43) was evaluated by X-ray fluorescence, and presented in *Table 2*, which shows the presence of 19.45% silica by weight and 52.55% CaO.

The XRD pattern shows the crystalline behavior of OPC along with the presence of dicalcium silicate, tri-calcium silicate, tri-calcium aluminate, tetra calcium alumino ferrite, and gypsum, which is shown in *Figure 2*.

Table 2 Chemical composition of OPC, FA, RHA, and SD

Compositions	Weight (%)			
	OPC (43 grade)	FA	RHA	SD
CaO	52.55	4.19	0.49	76.11
SiO_2	19.45	55.40	93.66	12.52
Al_2O_3	4.64	19.98	1.01	5.12
Fe_2O_3	3.23	6.82	1.02	3.61
MgO	2.15	2.03	1.05	-
K_2O	0.76	1.92	0.91	1.43
Na_2O	0.22	0.61	0.16	-
Loss on ignition	2.76	2.41	4.81	-

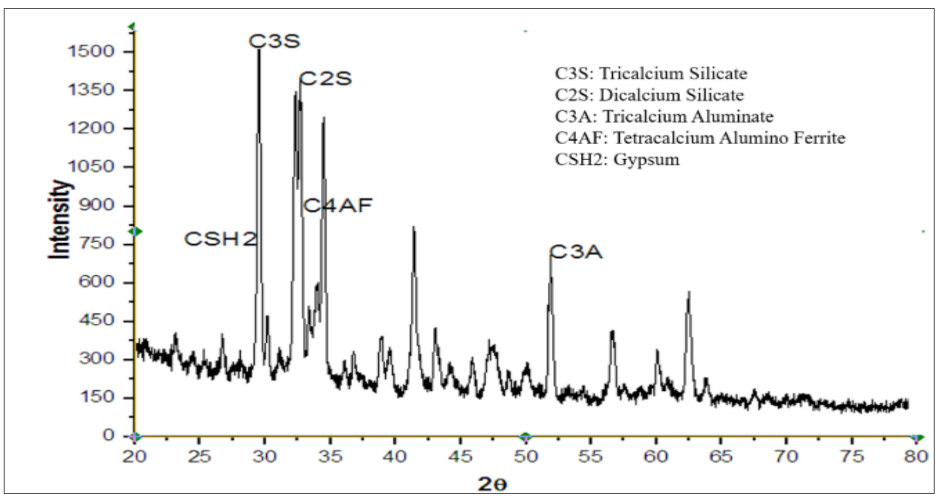

Figure 2 X-ray diffraction pattern of ordinary Portland cement (grade 43)

3.1.2Fly Ash (FA)

It was collected from National Thermal Power plant Corporation, Unchahar (25.9041°N, 81.3014°E), Uttar Pradesh, India. FA's chemical composition (*Table 2*) shows the presence of 55.40% silica, almost 20% alumina and nearly 7% ferrite. The physical properties of FA have been listed in *Table 3*.

Table 3 Physical properties of FA IS 3812:2013)

Parameters	**Value**
Specific gravity	2.13
Colour	Grey
Classification	f-class
Density	1000 kg/m3

The crystalline XRD x-ray diffraction pattern of FA has been shown in *Figure 3*, which confirms the presence of SiO_2, Al_2O_3, andFe_2O_3 compounds within it.

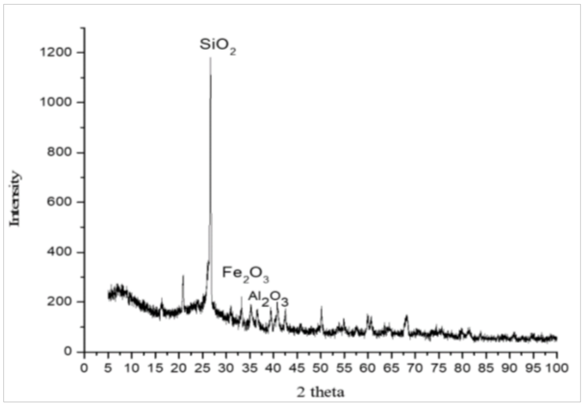

Figure 3 X-ray diffraction pattern of FA

Spherically shaped FA fly ash particles provide lubrication in the concrete mixture by acting as ball bearings, as shown in the microstructural scanning electron image *Figure 4(a).*

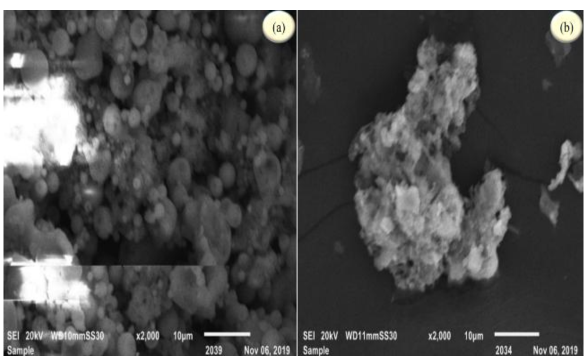

Figure 4 Microstructural images (SEM) of (a) FA and (b) RHA

3.1.3Rice husk ash (RHA)

It was purchased from Jalyan Trading in Anand, Gujarat, India. *Table 4* displays the physical characteristics of RHA. The chemical properties provided by the manufacturer itself are listed in *Table 2*. The FESEM image of RHA is shown in *Figure 4(b).*

Table 4 Characteristics of RHA

Properties	**Value**
Colour	Black
Specific surface area	15-18x10^4 cm^2/gm
Specific gravity	2.15

The XRD pattern of RHA has been presented in *Figure 5*, which shows the presence of kaolinite, illite, hematite, and silica compounds in RHA.

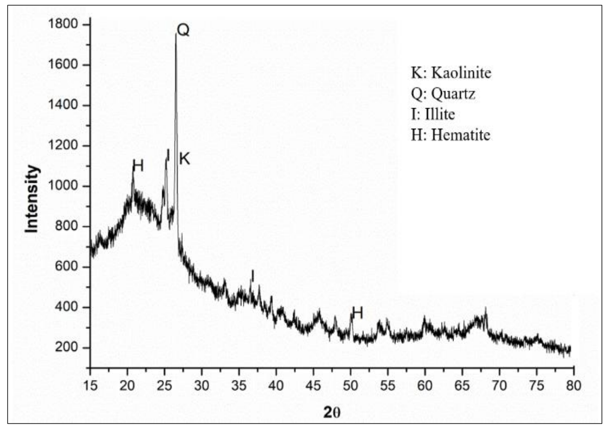

Figure 5 X-ray diffraction pattern of RHA

3.1.4Fine aggregate (N-sand)

All concrete samples were made using natural river sand that fulfils the criteria of zone II standards as per IS-383-1987. The physical properties of N-sand used in this study are shown in *Table 5*. The particle size distribution of fine aggregate and SD is presented in *Figure 6*, which lies in Zone-II as per IS 383-1970.

Table 5 Characteristics of N-sand, SD, and coarse aggregate

Properties	**N-sand**	**SD**	**Coarse aggregate**	
			10 mm	**20 mm**
Fineness modulus	2.462	2.32	6.25	7.27
Bulk density (kg/m3)	1680	NA	1590	1560
Specific gravity	2.48	2.35	2.67	2.70
Water absorption (%)	1.76	50	1.20	1.10

3.1.5Stone dust (SD)

SD of a grey hue was collected from stone-crushing facilities in Prayagraj, Uttar Pradesh. Before preparing the specimen, it was utterly air-dried and retained on an IS 150µm sieve. SD's physical characteristics are displayed in *Table 5*. The chemical composition is presented in *Table 2.*

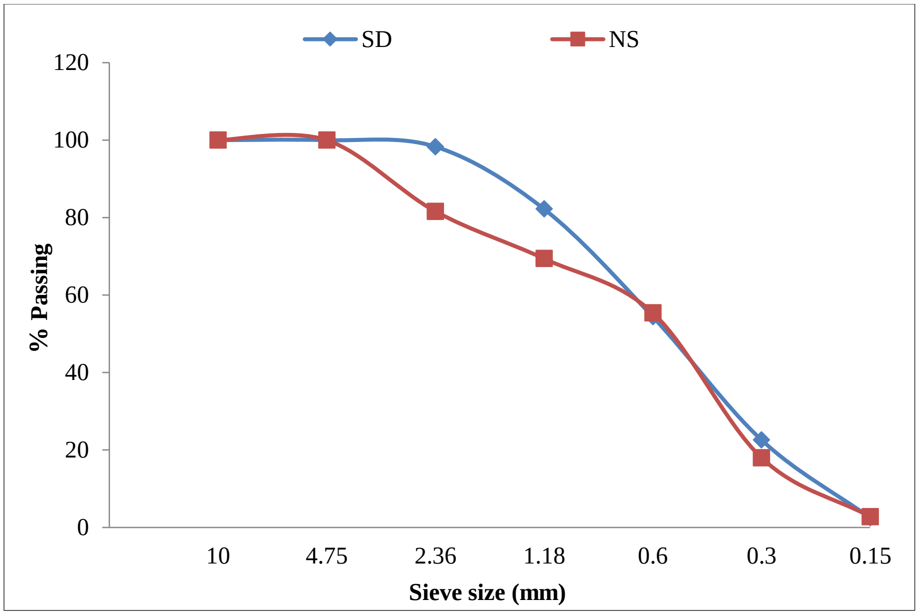

Figure 6 Particle size distribution of NS and SD

3.1.6Coarse aggregate

The size of coarse aggregate used in this study was 10 and 20 mm as per IS 383:1987. Aggregates should be clean, hard, and free from dirt and other impurities. The physical parameters of coarse aggregate have been presented in *Table 5.*

3.2Experimental program

The concrete mix was prepared using a constant water/binder ratio of 0.44 and a total binder content of 450 Kg/m^3. The quantity of fine aggregate, coarse aggregate, and superplasticizer dosage were 900 Kg/m^3, 828 Kg/m^3, and 5.85 Kg/m^3, respectively. After that, for the optimization of FA, RHA, and SD proportions in the design mix, standard cubes were prepared, cured for 28 days in tap water, and tested for the evaluation of compressive strength. Concrete cubes' compressive strength was determined using a compression testing machine (CTM) in structure analysis laboratory in Motilal Nehru National Institute Allahabad, Prayagraj with a capacity of 2000 kN. The load was applied at approximately 140 kg/cm^2/min, and to calibrate the CTM, a load was applied to a sample with known strength as per the provisions contained in IS: 516-1959. For the optimization of FA and FA+RHA, different mixes were prepared for different OPC replacement levels by FA, RHA, and FA+RHA. The replacement level of OPC with FA was- 5, 10, 15, 20, and 25% by mass. The obtained compressive strength is maximum when the replacement level of OPC is 20% FA. After that, for each replacement level of OPC with FA, the replacement level of RHA was also varied from 0-15% at an interval of 5%. Compressive strength obtained is maximum when the combined replacement level of OPC by FA and RHA is 20% and 5%, respectively. After optimization of fine aggregate, from 900 kg of fine aggregate, it was replaced by SD at 10, 20, 30, 35, and 40% by weight. The combination of 65% N-sand and 35% SD gives the maximum compressive strength value; therefore, these values were used further. From these proportions, three specimens of SCC were prepared, as listed in *Table 6*, for further study in terms of durability and microstructural analysis. Each test was performed three times for each specimen containing three samples. The average value was reported in this study. The result indicated reproducibility within the range of ±3%.

Table 6 Details of specimen for analysis

Specimens	Combination
SCC-I	80% OPC + 20% FA + 100 N-sand
SCC-II	75% OPC + 20% FA + 5% RHA + 100% N-sand
SCC-III	75% OPC + 20% FA + 5% RHA + 65% N-sand + 35% SD

For the optimization of FA, RHA, and SD proportions in the design mix, standard cubes were prepared, cured for 28 days in tap water as shown in *Figure 7(a)*, and tested for the evaluation of compressive strength. After 28 days, the specimens were fully submerged in ammonium sulphate [$(NH_4)_2SO_4$] solution having a concentration of

4.0 gram per litre, as shown in *Figure 7(b)*, for periods of 56 and 360 days to analyze the micro-structural characteristics and different durability aspects of these specimens.

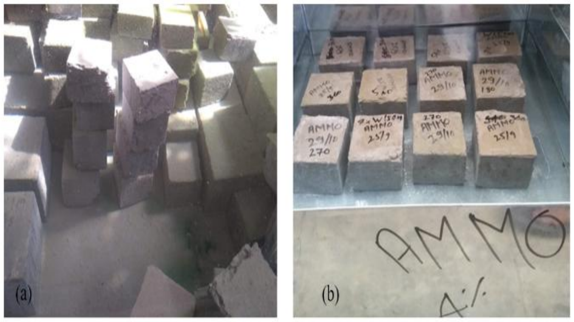

Figure 7 Curing of SCC specimens (a) in tap water and (b) in sulphate solution

The specimen was tested to evaluate its compressive strength by IS: 516 (1) 1959. Three samples from each specimen were weighed before being exposed to tap water and $(NH_4)_2SO_4$ solution to calculate the weight change. The mass of the specimens was again weighted following the necessary exposure time. Calculations were made for changes in specimens' weight at designated intervals. The specimen's sorptivity was also assessed per American Society for Testing and Materials (ASTM) C 1585. The microstructural behaviour was investigated using energy-dispersive spectroscopy (EDS), XRD, and elemental mapping (EM).

4.Results

4.1Fresh properties

Various concrete mixes' flowability and filling capacity were evaluated using the slump flow, as shown in *Figure 8(a)*, and V-funnel test, as shown in *Figure 8(b)*. The L-box, U-box, and J-ring tests assessed the concrete's passing capabilities, as shown in *Figure 8(c, d, & e)*.

It was discovered that SCC-I became more workable due to the spherical morphologies of the FA particles, while the rough surfaces of the RHA and SD particles slightly decreased the workability of SCC-II and SCC-III. Furthermore, it is found that adding FA improves the mixture's workability by utilizing some workability tests, such as L-box, U-box, slump flow, and J-ring [15, 40]. While the workability is somewhat reduced by adding RHA and SD as given in *Table 7*. Several researchers have also reported the same patterns in their findings [41].

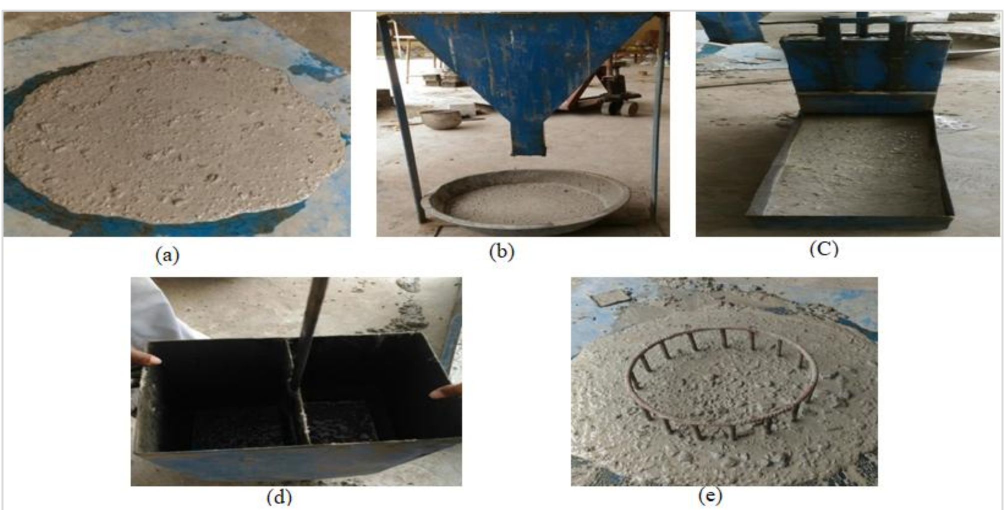

Figure 8 Workability of SCC samples carried out by (a) Slump flow, (b) V-funnel, (c) L-box, (d) U-box, and (e) J-ring

Table 7 Workability analysis of different specimens of SCC

Samples	Slump flow(mm)	V-funnel(sec.)	L-box(h_2/h_1)	U-box(mm)	J-ring(mm)
SSC-I	730	9.0	0.97	12.0	5.2
SSC-II	710	9.4	0.96	14.0	5.5
SSC-III	660	10.6	0.85	17.0	6.9
EFNARC (Codal provisions)	550 to 850	8 to 25	> 0.8	0 to 30	0 to 10

4.2 Hardened properties

The compressive strength of each specimen, submerged in tap water and in an $(NH_4)_2SO_4$ solution, was measured at different time intervals. The entire process was carried out at a room temperature of 27ºC ± 10ºC, and the results are presented in *Table 8*. Compressive testing machines undergo calibration through initial setup and inspection, standard calibration procedures, software, and mechanical adjustments, and repeat calibration. Validation includes routine maintenance and checks, inter-laboratory comparisons, proficiency testing, control specimens, and documentation.

Table 8 Compressive strength of samples in different exposure conditions

Curing period (Days)	Compressive strength (kN/m^2)					
	Tap water			Sulphate solution (4g/l)		
	SCC-I	SCC-II	SCC-III	SCC-I	SCC-II	SCC-III
28	44.67	45.67	46.67	44.67	45.67	46.67
56	47.00	48.67	48.67	46.33	48.00	48.00
180	50.00	51.33	51.33	49.00	50.00	50.33
270	51.33	52.67	52.67	49.67	51.00	51.33
360	52.00	53.33	53.33	50.00	51.67	52.00

4.3 Durability analysis

4.3.1 Changes in compressive strength of SCCs

The findings from water curing indicate that the specimens SCC-I, SCC-II, and SCC-III exhibit varying growth rates in compressive strength over time. When these samples are exposed to $(NH_4)_2SO_4$ solution curing, the compressive strength of samples also increases but at a slow growth rate compared with water curing. In SCC-I, the growth rate of compressive strength is less, as compared to SCC-II and SCC-III, because CSH gel formation is low. This means that the SCC-I shows more loss in compressive strength when exposed to sulphate solution. The sample SCC-III shows minimum loss during sulphate exposure because, during exposure, it produces more CSH gel, which further minimizes the voids between particles and increases the density. As a result, the CSH gel blocks the entry of sulphate molecules within the concrete due to reduced porosity. All the samples, i.e., SCC-I, SCC-II, and SCC-III, while exposed in sulphate solution exposure, show that the loss in the compressive strength increases at different growth rates with exposure time, i.e., 56, 180, 270, and 360 days as shown in *Figure 9*.

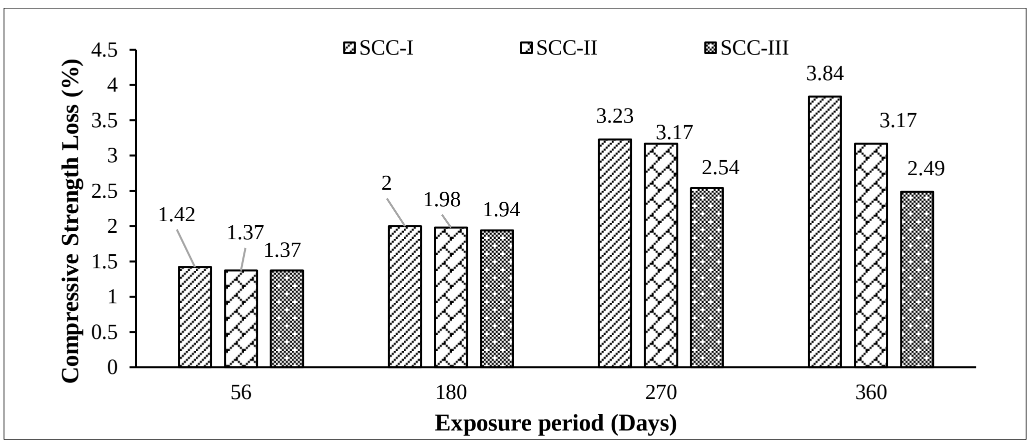

Figure 9 Loss in compressive strength with exposure periods

4.3.2 Variation in weight

The variation in weight of the samples exposed to the $(NH_4)_2SO_4$ solution over different time periods—28, 56, 90, 180, 270, and 360 days—is presented in *Table 9*. It has been observed that the weight of the samples SCC-I, SCC-II, and SCC-III has increased during the first 90 days of exposure, as shown in *Figure 10*. The weight increase might be due to various reactions, such as absorption and deposition of some foreign particles on the surface of the concrete. After 90 days, the weight of the samples has been found to decrease in order due to the leaching action that might be taking place by the surrounding sulphate solution.

Table 9 Weight of different samples in $(NH4)_2SO_4$ solution exposure (4g/l) conditions

Curing period (Days)	Weight of samples (kg)		
	SCC-I	**SCC-II**	**SCC-III**
28	2.583	2.558	2.611
56	2.610	2.584	2.637
90	2.614	2.586	2.638
180	2.611	2.585	2.637
270	2.610	2.584	2.637
360	2.609	2.578	2.637

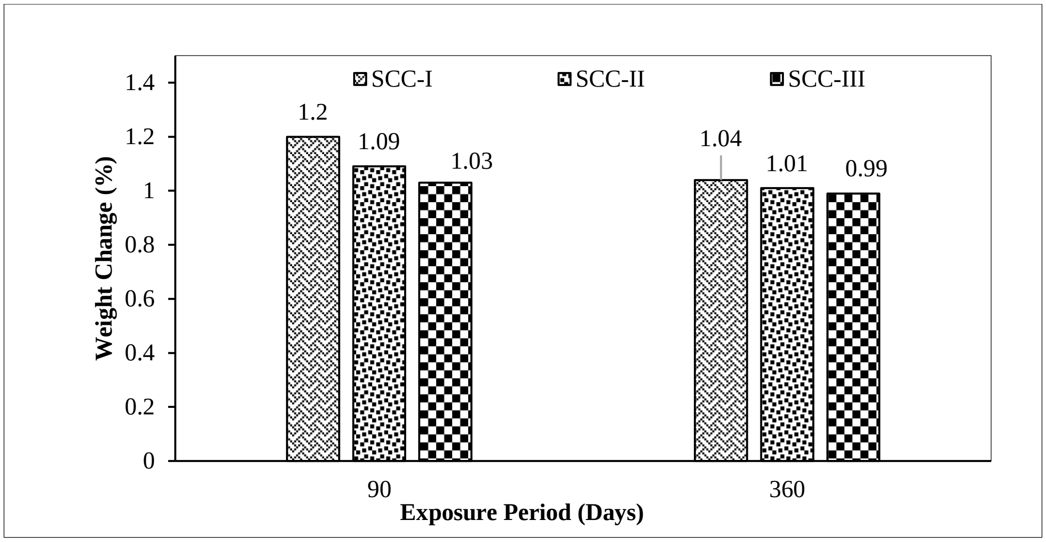

Figure 10 Change in weight with exposure periods

4.4Measurement of sorptivity

A sorptivity test was conducted in accordance with the guidelines of ASTM C 1585 to determine the capillary rise capacity in concrete specimens. By measuring the increase in mass of a specimen as a function of time when only one surface of the specimen is exposed to water ingress of unsaturated concrete by capillary suction during initial contact with water, this test is used to determine the rate of absorption (or sorptivity) of water. As shown in *Figure 11*, the rate of sorption is determined by the slope of the best-fit line in the plot of absorption versus the square root of time.

Figure 11 Sorptivity test setup (a) core cutting, (b) sample preparation, and (c) sorptivity test

The sorptivity test was conducted using initial and secondary data for all three specimens, i.e., SCC-I, SCC-II, and SCC-III. Sorptivity has been observed to decrease with time, and when compared to samples

SCC-I and SCC-II, sample SCC-III's sorptivity value was lower. *Table 10* displays the sorptivity values for each of the three specimens as 56 and 360 days of exposure to tap water. Based on the experimentation, it can be determined that the sorptivity of the specimens decreases as the curing period increases.

Table 10 Values of sorptivity ($\times 10^{-3}$ mm/s) for several SCC specimens

Samples	**Curing period**	
	56 Days	**360 Days**
SCC-I	0.171	0.164
SCC-II	0.121	0.108
SCC-III	0.112	0.098

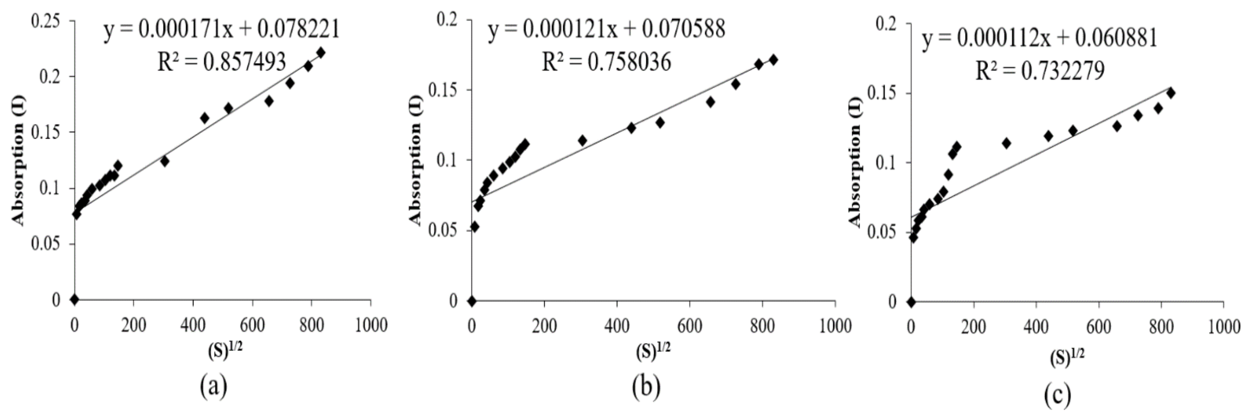

Figure 12 Sorptivity pattern after 56 days of water curing (a) SCC-I, (b) SCC-II, (c) SCC-III

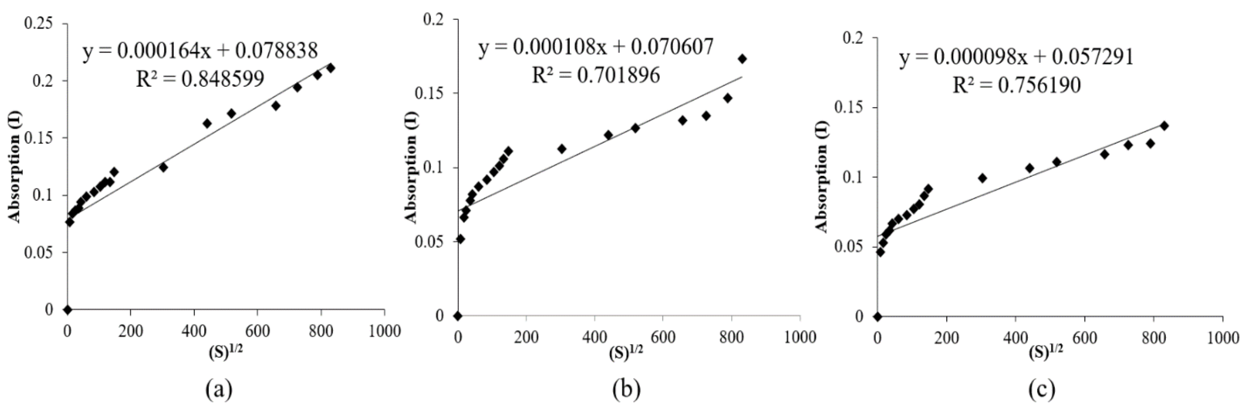

Figure 13 Sorptivity pattern after 360 days of water curing (a) SCC-I, (b) SCC-II, (c) SCC-III

4.5Variation in microstructural analysis

Microstructural analyses provide a comprehensive understanding of concrete's internal structure and composition. By linking these microscopic features to macroscopic properties, one can predict and improve the performance of concrete in various applications. High levels of crystalline phases, such as CSH, along with a homogeneous elemental distribution and increased density, signify enhanced strength, durability, and overall superior performance of concrete. After the specimens were cured in water and $(NH_4)_2SO_4$ solution for different periods, the XRD, EDS, and EM tests were carried out to analyse the internal microstructure of the specimen. An effective method for determining the different phases contained in a particular powered concrete mixture is assessed by XRD analysis, from which a specific crystalline phase in the concrete can be identified very accurately. Further, the relative amounts of the different phases in the sample can also be assessed through the relative intensities in the recorded X-ray diffractogram. The XRD study shows a lower peak for SCC-I and a higher peak for CSH in SCC-III.

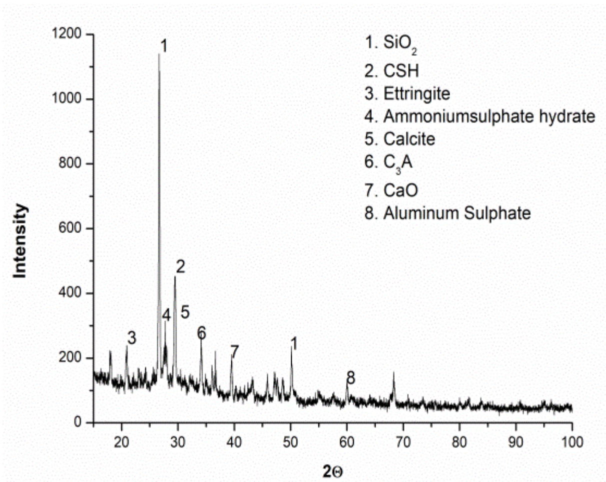

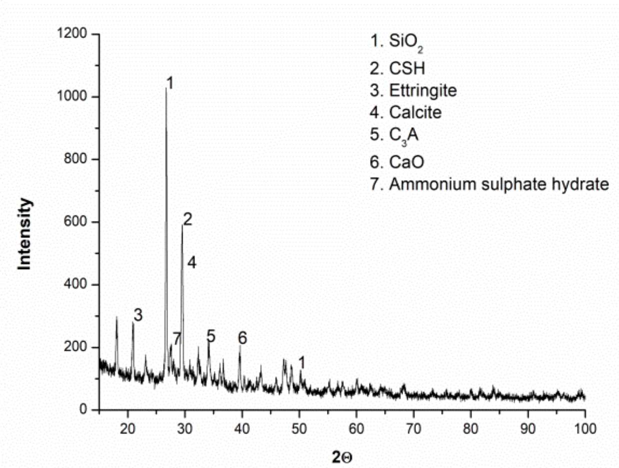

(a) (b)

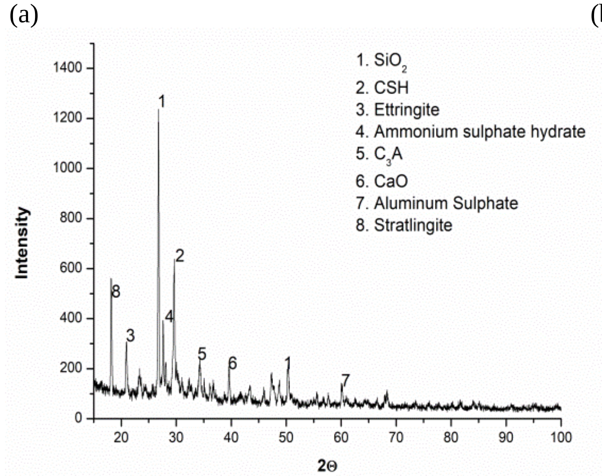

(c)

Figure 14 Water curing for a period of 56 days (a) SCC-I, (b) SCC-II, (c) SCC-III

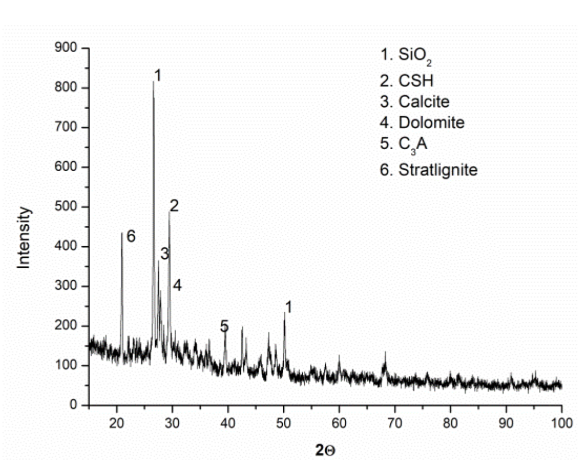

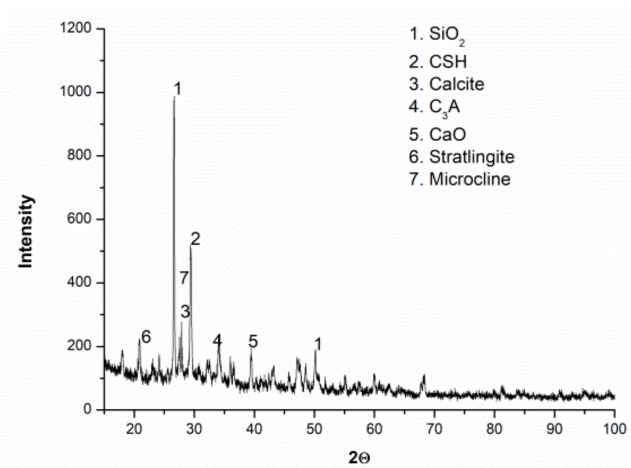

(a) (b)

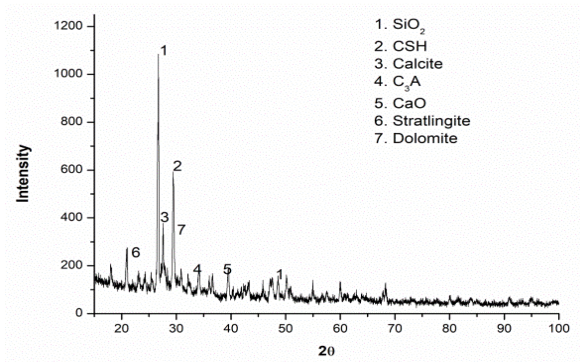

(c)

Figure 15 Water curing for a period of 360 days (a) SCC-I, (b) SCC-II, (c) SCC-III

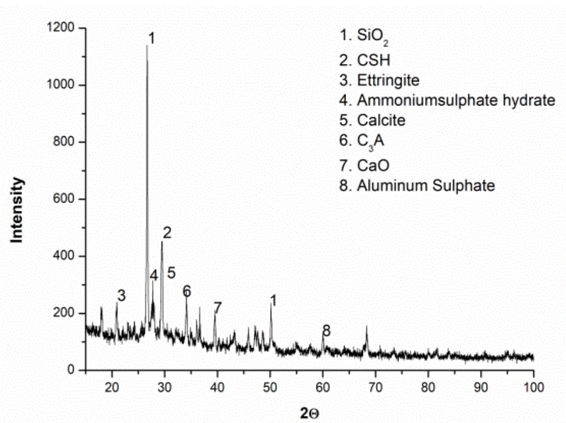

(a)

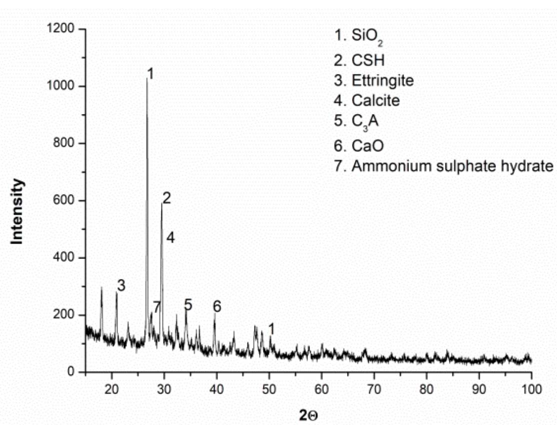

(b)

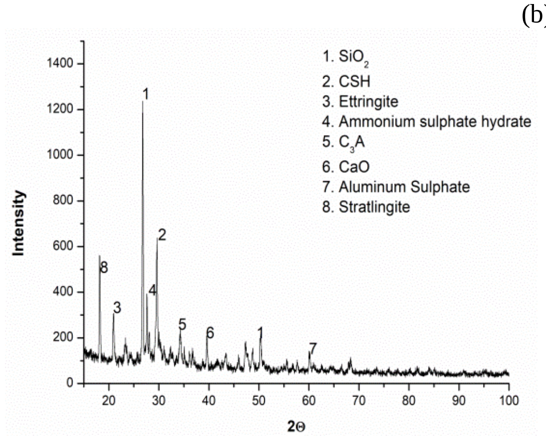

(c)

Figure 16 Curing in sulphate solution of 4g/l concentration for a period of 56 days (a) SCC-I, (b) SCC-II, (c) SCC-III

To verify the internal micro-structure of the SCC specimen discovered through the XRD pattern, the EDS and EM analyses were carried out for SCC-I, SCC-II, and SCC-III. The elemental alterations in the specimens cured in tap water for 56 and 360 days are shown in *Figures 18 to 19.* Similarly, the results for specimens exposed to a 4.0 g/l $(NH_4)_2SO_4$ solution for 56 and 360 days are presented in *Figures 20 to 21*. The related EDS spectra provide evidence of aluminum sulphate and ettringite development in specimens subjected to sulphate solution. Following a thorough XRD analysis of each specimen sample that was cured in tap water for up to 360 days, CSH, dicalcium silicate, SiO_2, stratlingite, calcium-aluminum-oxide-sulphate, gismondite, dolomite, calcite, tricalcium aluminate, etc., were discovered to be the most common compounds. CSH and Quartz peaks were highest in SCC-III specimens containing FA, RHA, and SD. The main reason for strength gain is the additional CSH gel created when FA is introduced. Additionally, the pore structure is refined by the tiny particles of these, making it more resilient to sulphate attack. The components quartz and CSH are visible in the XRD pattern of the specimens subjected to the $(NH_4)_2SO_4$ solution.

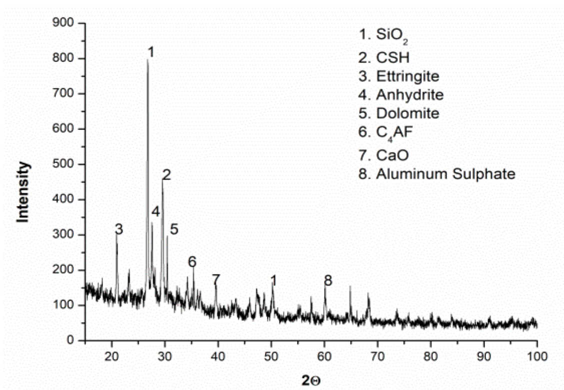

(a)

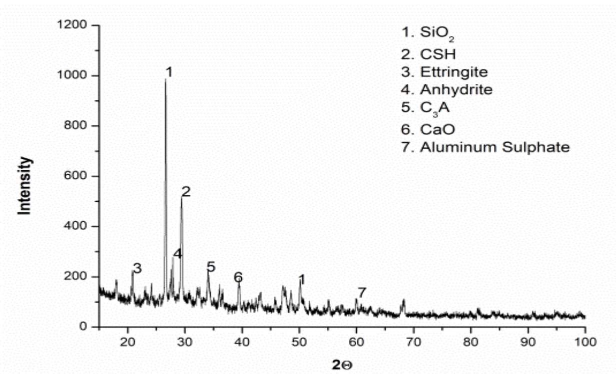

(b)

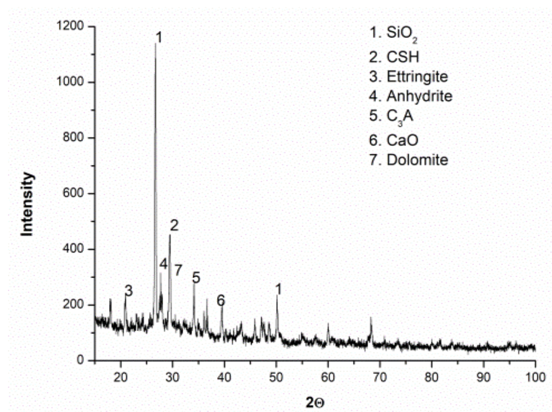

(c)

Figure 17 Curing in sulphate solution of 4g/l concentration for a period of 360 days (a) SCC-I, (b) SCC-II, (c) SCC-III

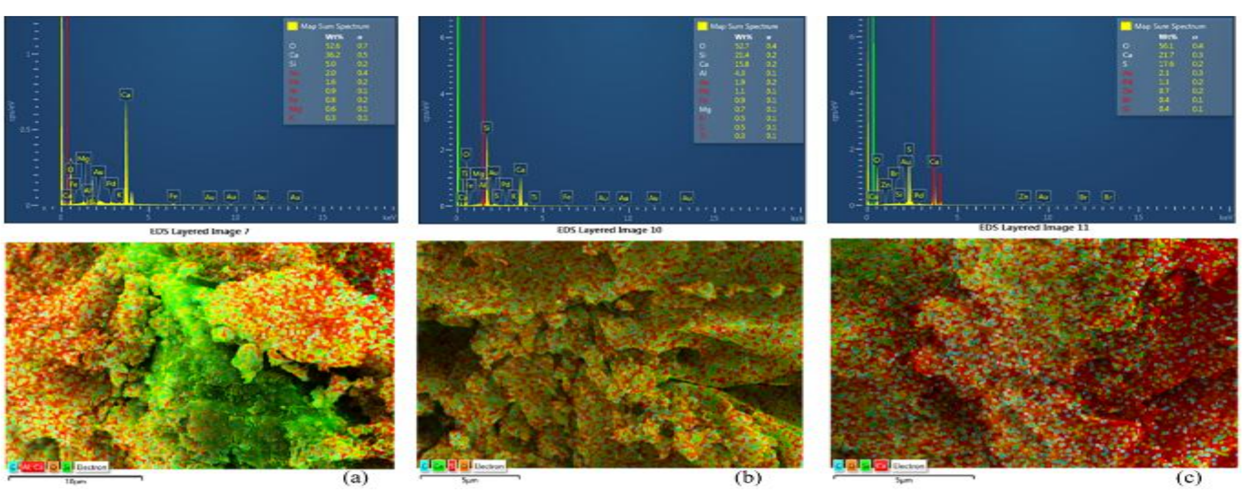

Figure 18 EDS and EM of (a) SCC-I, (b) SCC-II, (c) SCC-III samples in water curing for a period of 360 days

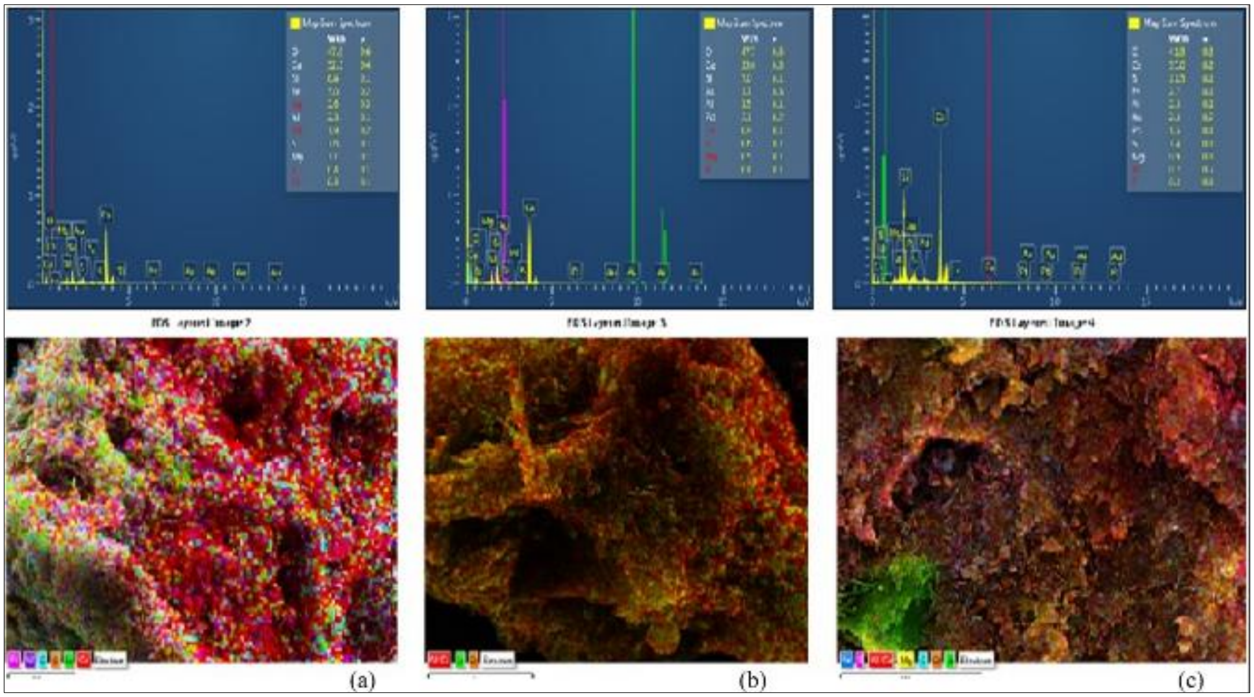

Figure 19EDS and EM of (a) SCC-I, (b) SCC-II, (c) SCC-III samples in water curing for 56 days

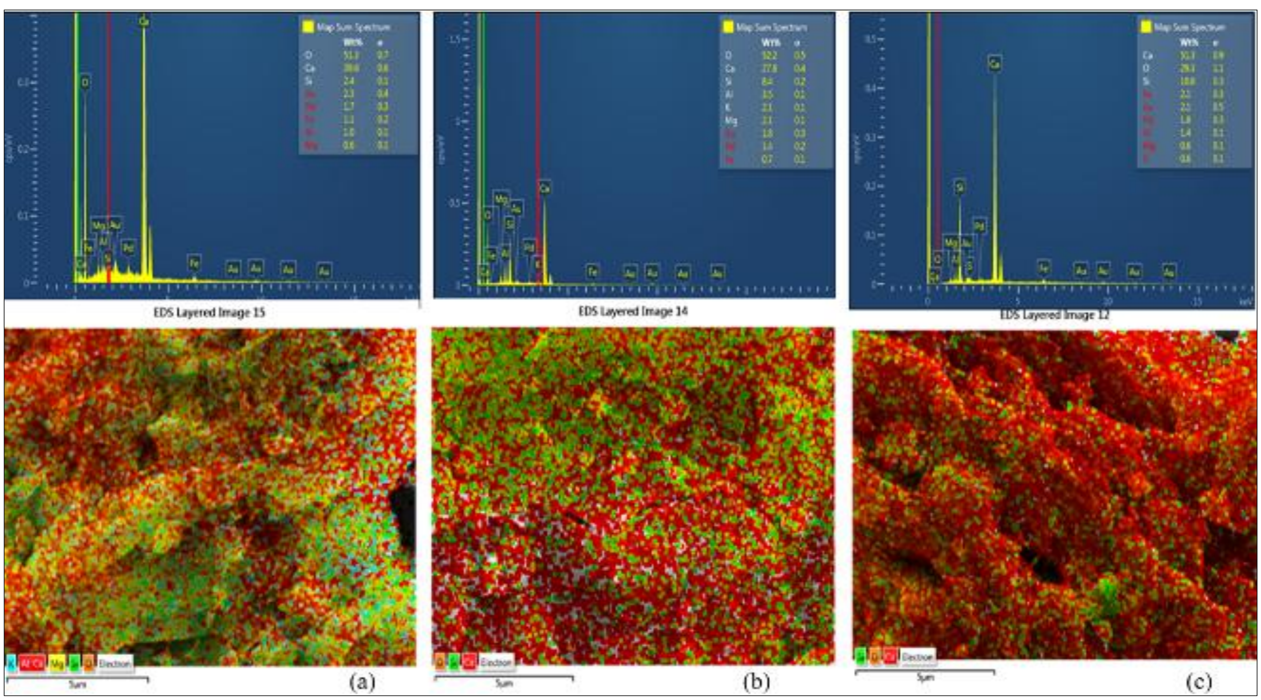

Figure 20 EDS and EM of (a) SCC-I, (b) SCC-II, (c) SCC-III samples exposed in sulphate solution of 4g/l concentration for 56 days

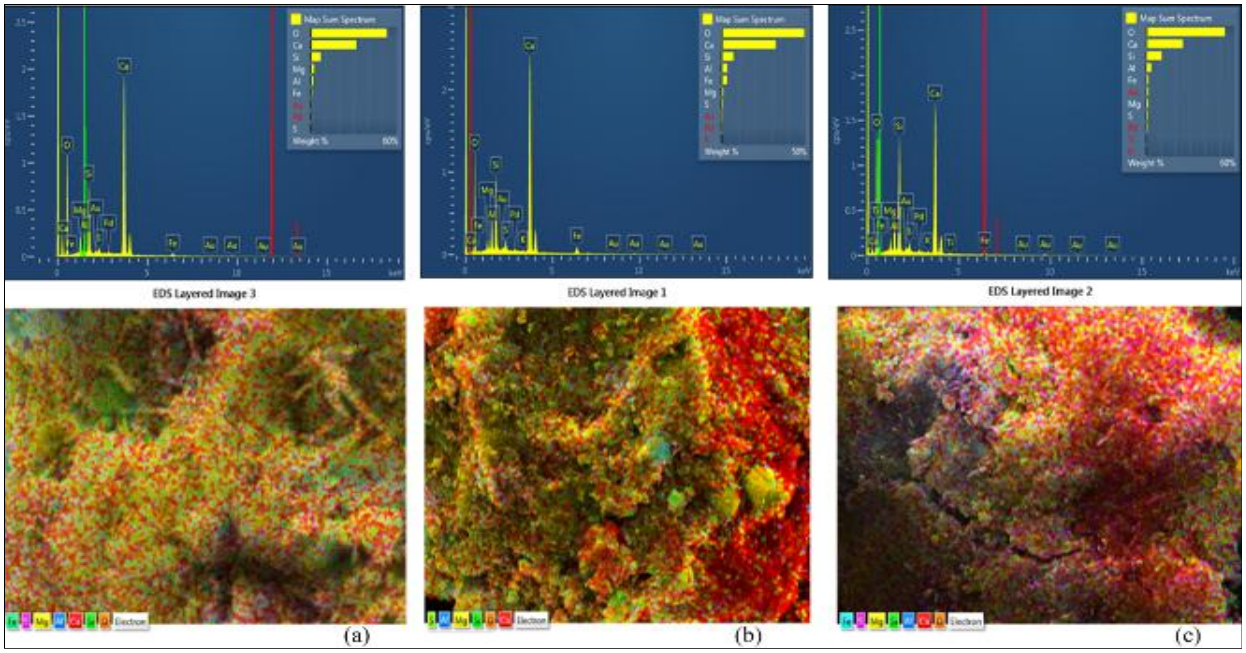

Figure 21 EDS and EM of (a) SCC-I, (b) SCC-II, (c) SCC-III samples exposed in sulphate solution of 4g/l concentration for 360 days

5.Discussion

5.1Fresh properties

The results of the fresh SCC mixtures, presented in *Table 7*, show that the slump flow ranges from 550 to 850 mm, meeting the flowability requirements specified by EFNARC [41]. The maximum slump flow was found for SCC-I, i.e., 730 mm. The V-funnel time of different mixes was in the range of 8-25 sec. L-box values, i.e., blocking ratio (h2/h1), were found in the range of 0.8-1.1, satisfying the requirement of EFNARC. The values of U-box (0-30mm) and J-ring (0-10mm) were also within the desirable limits of EFNAR. All the SCC mixes were found to satisfy the EFNARC limits.

The change in the slump flow is -70mm for SCC-III and -20mm for SCC-II. The change in the V-funnel value is +1.6 sec for SCC-III and +0.4 sec for SCC-II. The change in the L-box value is -0.12 mm for SCC-III and -0.01 mm for SCC-II. The change in the U-box value is +5 mm for SCC-III and +2.0 mm for SCC-II. The change in the J-ring value is +1.7 mm for SCC-III and +0.3 mm for SCC-II as compared to SCC-I.

5.2Hardened properties

Compared to SCC-I's compressive strength after 28 days, the strength gains of SCC-I, SCC-II, and SCC-III at 360 days are approximately 16.40, 19.38, and 19.38%, respectively. The increase in compressive strength for SCC-I, SCC-II, and SCC-III ranged between 1–6.40%, 1–6.77%, and 1–4.27%, respectively, when cured in tap water for up to 360 days compared to their strength at 28 days of curing. After 28 days of curing in tap water, SCC-II and SCC-III exhibited strength gains of approximately 2.23% and 4.47%, respectively, over SCC-I. These improvements can be attributed to the high pozzolanic activity, high reactivity, and fine particle sizes of FA and RHA, which likely facilitated the formation of stronger bonds among the concrete constituents [42, 43].

5.3Durability analysis

5.3.1Changes in compressive strength of SCCs

As observed in *Figure 9*, after 360 days of exposure to the sulphate solution (4.0 g/l), the compressive strength loss is 3.84%, 3.17%, and 2.49% for S-1, S-2, and S-3 mixes, respectively, compared to their strength at 28 days. Among the samples, SCC-III exhibits the minimum strength loss, outperforming SCC-I and SCC-II in resistance to sulphate exposure.

5.3.2Variation in weight

The percentage weight change of SCC-I, SCC-II, and SCC-III specimens exposed to a 4.0 g/l sulphate solution is presented in *Figure 10*. It is observed that the cube weights increase up to 90 days of exposure, likely due to absorption and deposition of reaction products, after which a gradual decrease in weight is observed. In a 4.0 g/l salt solution, the largest gain recorded is 1.2% at 90 days in SCC-I, while the minimum gain is 0.99% at 360 days. The mass gain might be due to the reaction product deposition and solution absorption inside the specimen's surface.

5.3.3Measurement of sorptivity

As shown in *Table 10*, after 56 days of exposure, the sorptivity of SCC-III decreased by 7.43% and 34.50% compared to SCC-II and SCC-I, respectively. After 360 days, the sorptivity of SCC-III was 9.25% and 40.24% lower than that of SCC-II and SCC-I, respectively. *Figure 12* and *Figure 13* show the sorptivity plot for all three samples of SCC after tap-water curing at 56 and 360 days. To calculate the sorptivity, the slope of the best-fitting curve in the absorption vs. square root of the time plot was utilized. There might have been a more significant absorption rate at the beginning of the test because the early portion of the curve (up to 6 hours) had a steeper slope than the later portion (1 to 7 days).

When comparing SCC-III to SCC-II and SCC-I, a greater improvement was seen. For SCC-III specimens containing FA, RHA, and SD, the least sorptivity found improves the concrete's pore structure. When comparing the sorptivity of the SCC-I, SCC-II, and SCC-III specimens at 360 days after curing in tap water to their sorptivity at 56 days, the improvements are 4.09, 10.70, and 12.5%, in that order.

5.3.4Variation in microstructural analysis

The XRD results of the SCC specimens, shown in *Figures 14* to *17*, reveal the presence of potassium-aluminum-sulphate-hydrate, CSH, SiO_2, $(NH_4)_2SO_4$, CH, ettringite, and stratlingite. After exposure to the sulphate solution, SCC-I showed larger peaks of ettringite than SCC-II and SCC-III. The expansion in concrete is mostly caused by ettringite, gypsum, and brucite intensities, all of which were less in the SCC-II and SCC-III specimens after they were subjected to the sulphate solution. *Figures 18 to 21* also show the EDS and EM examination of the corresponding specimen following 56 and 360 days of exposure to tap water and sulphate solution (4.0 g/l). The elements Si, Ca, O, H, and S have been identified from the EDS and EM graphs. It demonstrates that a greater abundance of the element Si is present in SCC-II and SCC-III in contrast to SCC-I. The Ca: Si ratio is lower in specimens containing FA, RHA, and SD, which speeds up pozzolanic reactions and contributes to strength growth and increased resistance to sulphate attack.

5.4Limitations

The current study aimed to evaluate the effects of incorporating FA, RHA, and SD in the production of SCC and their performance under sulphate exposure. Future research could explore the following:

- The impact of adding various mineral admixtures (e.g., silica fume, metakaolin, ground granulated blast furnace slag), fibers (e.g., steel, glass), and aggregates (e.g., manufactured sand, recycled aggregates) on the fresh and mechanical properties of SCC.
- A more comprehensive examination of durability aspects through tests such as abrasion resistance, carbonation, rapid chloride penetration test (RCPT), and exposure to different salts and acids (e.g., chloride, nitrate).

Appendix I has a comprehensive list of abbreviations.

6.Conclusion and future work

FA, RHA, and SD can be used in the following proportions to produce SCC-III: 20%, 5%, and 35%, respectively. The addition of FA enhances the flowability of SCC mixtures, while the inclusion of N-sand and RHA results in a slight reduction in flowability. After 28 days of tap-water curing, SCC-II and SCC-III exhibited greater compressive strength compared to SCC-I. Over a 360-day exposure period, SCC-I showed a higher compressive strength loss (3.80%) than SCC-II (3.11%) and SCC-III (2.49%).

In a 4.0 g/l sulphate solution, the weight of SCC specimens increased over the first 90 days, reaching maximum weight variations of 1.20%, 1.09%, and 1.03% for SCC-I, SCC-II, and SCC-III, respectively. However, beyond 90 days, a reduction in weight was observed, with SCC-I, SCC-II, and SCC-III showing weight variations of 1.04%, 1.01%, and 0.99%, respectively, after 360 days. The sorptivity of the specimens decreased as the curing period increased, with SCC-III, which incorporates FA, RHA, and SD, demonstrating superior performance compared to SCC-I, which contains only FA. After 360 days of tap-water curing, SCC-III specimens exhibited a 12.5% improvement in sorptivity compared to their sorptivity at 56 days. Furthermore, SCC-II and SCC-III specimens showed improvements in sorptivity of 34.14% and 40.24%, respectively, compared to SCC-I, indicating that the combination of FA, RHA, and SD enhances sorptivity.

XRD analysis revealed that specimens exposed to sulphate solutions generated ettringite, aluminium sulphate, and ammonium sulphate hydrate, with these compounds being more prevalent in SCC-I than in SCC-II and SCC-III. The morphological and elemental content of the compounds were further analyzed using EDS and EM, corroborating the XRD data.

Acknowledgment
The authors sincerely acknowledge the Advanced Centre for Material Science, IIT Kanpur, for providing access to X-ray diffraction, Elemental Mapping, Energy Dispersive X-ray Spectroscopy, and FESEM facilities. Additionally, they express their gratitude to the Centre for Interdisciplinary Research, MNNIT Allahabad, for providing the X-ray diffraction facility.

Conflicts of interest
The authors have no conflicts of interest to declare.

Data availability
None.

Author's contribution statement
Amrendra Singh: Investigation, Methodology, Visualization, Writing – original draft, **Rakesh Kumar:** Conceptualization, Visualization, Supervision, Writing – review & editing, **P. K. Mehta:** Supervision, Visualization, Writing – review & editing, **Pawan Kumar:** Writing – original draft, Data curation, Writing –curation, Writing – review & editing.

References

[1] Jin R, Chen Q. An investigation of current status of "green" concrete in the construction industry. In 49th ASC annual international conference proceedings 2013 (pp. 1-8).

[2] Rashid S, Singh M. An investigation on carbon dioxide incorporated sustainable ready-mix concrete using OPC and PPC. Arabian Journal for Science and Engineering. 2023; 48(10):14213-36.

[3] Gao T, Shen L, Shen M, Liu L, Chen F, Gao L. Evolution and projection of CO_2 emissions for China's cement industry from 1980 to 2020. Renewable and Sustainable Energy Reviews. 2017; 74:522-37.

[4] Sukmak P, Sukmak G, Horpibulsuk S, Setkit M, Kassawat S, Arulrajah A. Palm oil fuel ash-soft soil geopolymer for subgrade applications: strength and microstructural evaluation. Road Materials and Pavement Design. 2019; 20(1):110-31.

[5] Ding GK. Sustainable construction-the role of environmental assessment tools. Journal of Environmental Management. 2008; 86(3):451-64.

[6] Fernando A, Selvaranjan K, Srikanth G, Gamage JC. Development of high strength recycled aggregate concrete-composite effects of fly ash, silica fume and rice husk ash as pozzolans. Materials and Structures. 2022; 55(7):1-22.

[7] Bahoria BV, Parbat DK, Nagarnaik PB. XRD analysis of natural sand, quarry dust, waste plastic (ldpe) to be used as a fine aggregate in concrete. Materials Today: Proceedings. 2018; 5(1):1432-8.

[8] https://environmentclearance.nic.in/writereaddata/SandMiningManagementGuidelines2016.pdf. Accessed 22 December 2024.

[9] Dey S, Kumar VP, Goud KR, Basha SK. State of art review on self compacting concrete using mineral admixtures. Journal of Building Pathology and Rehabilitation. 202; 6(1):18.

[10] Diop B, Mélinge Y, Molez L, Jauberthie R, Bouguerra A. Durability of mortars with natural fillers in aggressive environnement. In structural faults and repair 2008 (pp.1-8). HAL Open Science.

[11] Shokravi H, Mohammadyan-yasouj SE, Koloor SS, Petrů M, Heidarrezaei M. Effect of alumina additives on mechanical and fresh properties of self-compacting concrete: a review. Processes. 2021; 9(3):1-22.

[12] Singh A, Mehta PK, Kumar R. Recycled coarse aggregate and silica fume used in sustainable self-compacting concrete. International Journal of Advanced Technology and Engineering Exploration. 2022; 9(96):1581-96.

[13] Busari AA, Akinmusuru JO, Dahunsi BI. Review of sustainability in self-compacting concrete: the use of waste and mineral additives as supplementary cementitious materials and aggregates. Portugaliae Electrochimica Acta. 2018; 36(3):147-62.

[14] Adebakin IH, Gunasekaran K, Annadurai R. Mechanical properties of self-compacting coconut shell concrete blended with fly ash. Asian Journal of Civil Engineering. 2019; 20:113-24.

[15] Bouzoubaâ N, Lachemi M. Self-compacting concrete incorporating high volumes of class F fly ash: preliminary results. Cement and Concrete Research. 2001; 31(3):413-20.

[16] Yao ZT, Ji XS, Sarker PK, Tang JH, Ge LQ, Xia MS, et al. A comprehensive review on the applications of coal fly ash. Earth-Science Reviews. 2015; 141:105-21.

[17] Hossain SS, Mathur L, Roy PK. Rice husk/rice husk ash as an alternative source of silica in ceramics: a review. Journal of Asian Ceramic Societies. 2018; 6(4):299-313.

[18] Kosior-kazberuk M, Lelusz M. Strength development of concrete with fly ash addition. Journal of Civil Engineering and Management. 2007; 13(2):115-22.

[19] Tripathi D, Kumar R, Mehta PK. Development of an environmental-friendly durable self-compacting concrete. Environmental Science and Pollution Research. 2022; 29(36):54167-80.

[20] De MPR, Foiato M, Prudêncio JLR. Ecological, fresh state and long-term mechanical properties of high-volume fly ash high-performance self-compacting concrete. Construction and Building Materials. 2019; 203:282-93.

[21] Patil S, Ramesh B, Sathish T, Saravanan A, Almujibah H, Panchal H, et al. Evaluation and optimization of mechanical properties of laterized concrete containing fly ash and steel fiber using Taguchi robust design method. Alexandria Engineering Journal. 2024; 87:682-706.

[22] Rao MD, Dey S, Rao BP. Characterization of fiber reinforced self-compacting concrete by fly ash and cement. Chemistry of Inorganic Materials. 2023; 1:1-14.

[23] Mohammed AM, Asaad DS, Al-hadithi AI. Experimental and statistical evaluation of rheological properties of self-compacting concrete containing fly ash and ground granulated blast furnace slag. Journal of King Saud University-Engineering Sciences. 2022; 34(6):388-97.
[24] Mohamed OA, Najm O, Ahmed E. Alkali-activated slag & fly ash as sustainable alternatives to OPC: sorptivity and strength development characteristics of mortar. Cleaner Materials. 2023; 8:1-21.
[25] Abellan-garcia J, Martinez DM, Khan MI, Abbas YM, Pellicer-martínez F. Environmentally friendly use of rice husk ash and recycled glass waste to produce ultra-high-performance concrete. Journal of Materials Research and Technology. 2023; 25:1869-81.
[26] Ahmadi MA, Alidoust O, Sadrinejad I, Nayeri M. Development of mechanical properties of self compacting concrete contain rice husk ash. International Journal of Computer, Information, and Systems Science, and Engineering. 2007; 1(4):168-71.
[27] Anjos MA, Camões A, Campos P, Azeredo GA, Ferreira RL. Effect of high volume fly ash and metakaolin with and without hydrated lime on the properties of self-compacting concrete. Journal of Building Engineering. 2020; 27:100985.
[28] Tayeh BA, Hakamy AA, Fattouh MS, Mostafa SA. The effect of using nano agriculture wastes on microstructure and electrochemical performance of ultra-high-performance fiber reinforced self-compacting concrete under normal and acceleration conditions. Case Studies in Construction Materials. 2023; 18:1-17.
[29] Mosaberpanah MA, Umar SA. Utilizing rice husk ash as supplement to cementitious materials on performance of ultra high performance concrete–a review. Materials Today Sustainability. 2020; 7:100030.
[30] Venkatanarayanan HK, Rangaraju PR. Material characterization studies on low-and high-carbon rice husk ash and their performance in Portland cement mixtures. Advances in Civil Engineering Materials. 2013; 2(1):266-87.
[31] Jongpradist P, Homtragoon W, Sukkarak R, Kongkitkul W, Jamsawang P. Efficiency of rice husk ash as cementitious material in high-strength cement-admixed clay. Advances in Civil Engineering. 2018; 2018(1):1-11.
[32] Rahman ME, Nagaratnam BH, Pakrashi V, Muntohar AS, Sujan D, Chai N, et al. A preliminary study on self compacting concrete using RHA. In proceedings of the 3rd CUTSE international conference 2011 (pp. 495-500). Curtin University.
[33] Nayak DK, Abhilash PP, Singh R, Kumar R, Kumar V. Fly ash for sustainable construction: a review of fly ash concrete and its beneficial use case studies. Cleaner Materials. 2022; 6:1-35.
[34] Lakhani R, Kumar R, Tomar P. Utilization of stone waste in the development of value added products: a state of the art review. Journal of Engineering Science & Technology Review. 2014; 7(3):180-7.
[35] Hamid NJ, Kadir AA, Kamil NA, Hassan MI. Overview on the utilization of quarry dust as a replacement material in construction industry. International Journal of Integrated Engineering. 2018; 10(2):112-7.
[36] Singh SK, Srivastava V, Agarwal VC, Kumar R, Mehta PK. An experimental investigation on stone dust as partial replacement of fine aggregate in concrete. Journal of Academia and Industrial Research. 2014; 3(5):229-32.
[37] Eren Ö, Marar K. Effects of limestone crusher dust and steel fibers on concrete. Construction and Building Materials. 2009; 23(2):981-8.
[38] Bh AR, JE M. Impact of quarry dust and fly ash on the fresh and hardened properties of self compacting concrete. International Research Journal of Engineering and Technology. 2015; 2(8):786-95.
[39] Uygunoğlu T, Topçu İB, Çelik AG. Use of waste marble and recycled aggregates in self-compacting concrete for environmental sustainability. Journal of Cleaner Production. 2014; 84:691-700.
[40] Pathak N, Siddique R. Properties of self-compacting-concrete containing fly ash subjected to elevated temperatures. Construction and Building Materials. 2012; 30:274-80.
[41] Wang HY, Huang WL. Durability of self-consolidating concrete using waste LCD glass. Construction and Building Materials. 2010; 24(6):1008-13.
[42] Singh A, Kumar R, Mehta PK, Tripathi D. Mechanical performance of self-compacting concrete with pozzolanic material. In recent advances in structural engineering: select proceedings of NCRASE 2020 (pp. 11-20). Springer Singapore.
[43] Singh A, Kumar R, Mehta PK, Tripathi D. Properties of binary admixture mixed SCC exposed to sulphate environment. In sustainable building materials and construction: select proceedings of ICSBMC 2022 (pp. 129-36). Singapore: Springer Nature Singapore.

Mr. Amrendra Singh is a Research Scholar in the Civil Engineering Department, MNNIT Allahabad, Prayagraj, UP, India. He completed his B.Tech. in Civil Engineering from UPTU Lucknow in 2014 and M.Tech. in Structural Engineering from MNNIT Allahabad, Prayagraj in 2017. He has over 20 research papers published in reputable national and international journals and conferences. His areas of research include Concrete Technology, Composite Materials, Building Materials, Micro-Structural Analysis of Materials, and Structural Analysis.
Email: amrendra@mnnit.ac.in

Dr. Rakesh Kumar is a Civil Engineering Professor at MNNIT Allahabad in Prayagraj, Uttar Pradesh, India. In 1991, he completed his B.Tech. in Civil Engineering from IET Lucknow, M.Tech. in Structural Engineering from the Faculty of Engineering and Technology, Baroda, in 1993, and Ph. D. from IIT, BHU, Varanasi in 2001. Until now, he has organized more than ten short-term courses/workshops. He is a life member of the Chennai-based Indian Concrete Institute. He has over 100 research papers published in reputable national and international journals and conferences. Concrete technology, Composite Materials, and Waste Material Utilisation in the Construction Industry are among his areas of interest.
Email: rkpat@mnnit.ac.in

Dr. P. K. Mehta is a Professor of Civil Engineering at MNNIT Allahabad in Prayagraj, Uttar Pradesh, India. He completed his BE from MNREC, Allahabad, in 1986 and received his MTech & PhD from IIT, BHU, in 1991 & 1996, respectively. He is a life member of IIT Roorkee's Indian Society for Construction Material and Structures (ISCMS) and New Delhi's Swadeshi Science Movement. He has over 100 research papers published in prestigious national and international journals and conferences. Concrete Technology, Bridges, and Structures are among his areas of interest.
Email: pradeep11@mnnit.ac.in

Dr. Pawan Kumar is a Civil Engineering professional in Prayagraj, Uttar Pradesh. He completed his B. Tech. in Civil Engineering from UPTU Lucknow in 2013. He was awarded a Ph.D. degree in Civil engineering from MNNIT Allahabad in 2022. He has published more than 14 research papers in several national and international journals and conferences. He has been a life member of the Indian Geotechnical Society (IGS), New Delhi, since 2023.
Email: rce1652@mnnit.ac.in

Appendix I

S. No.	Abbreviations	Description
1	$(NH_4)_2SO_4$	Ammonium Sulphate
2	ASTM	American Society for Testing and Materials
3	CH	Calcium Hydroxide
4	CSH	Calcium Silicate Hydrate
5	CTM	Compression Testing Machine
6	EDS	Energy Dispersive Spectroscopy
7	EM	Elemental Mapping
8	FA	Fly Ash
9	GGBS	Ground Granulated Blast-Furnace Slag
10	MK	Metakaolin
11	NRSA	Nano Rice Straw Ash
12	N-Sand	Natural Sand
13	OPC	Ordinary Portland Cement
14	RHA	Rice Husk Ash
15	SCC	Self-Compacting Concrete
16	SCC-I	Self-Compacting Concrete made with 80% OPC, 20%FA, and 100%N-Sand
17	SCC-II	Self-Compacting Concrete made with 80% OPC, 20%FA, 5% RHA, and 100%N-Sand
18	SCC-III	Self-Compacting Concrete made with 80% OPC, 20%FA, 5% RHA, 65%N-Sand and 35%SD
19	SF	Silica Fume
20	SD	Stone Dust
21	SEM	Scanning Electron Microscopy
22	SP	Superplasticizers
23	UHPC	Ultra-High-Performance Concrete
24	w/b	Water/Binder
25	XRD	x-Ray Diffraction